Journal of Thermal Analysis and Calorimetry (2023) 148:5387–5394
https://doi.org/10.1007/s10973-023-12061-z

Isotherm kinetics of PIP2 bound gelsolin inactivation

Dávid Szatmári[1] · **Dénes Lőrinczy**[1]

Received: 8 December 2022 / Accepted: 26 February 2023 / Published online: 20 March 2023

Abstract
Actin monomers (G-actin) and filaments (F-actin) have dynamical rearrangement thus manage cellular motility, division and transport processes. The gelsolin (GSN) regulates the remodeling of cytoskeleton. After the activation of GSN by calcium ions, it can sever actin filaments then capped at its barbed end. In the cytoplasm, GSN manages the cellular motions and morphology. Phosphatidylinositol 4,5-bisphosphate (PIP2) is involved in signal transduction and the regulation of the actin cytoskeleton by regulation of actin-binding proteins. GSN can bind to PIP2 and thus can be localized in the near of the plasma membrane and released from the end of F-actin. We test here with isoperibol calorimetry the enthalpy change, within the interplay between GSN and F-actin under nano-, micro- and millimolar calcium concentrations and express the importance of PIP2 binding for the inactivation of GSN. As we have demonstrated here that PIP2 binding stabilizes the structure of gelsolin and reduces its actin monomer binding activity under nanomolar calcium as the typical cytoplasmic calcium concentration of resting cells. The gelsolin shows partial activity under micromolar and total activity with strong responses under millimolar calcium. If gelsolin-capped filaments point at the plasma membrane helps the binding between gelsolin and PIP2, and hence, filament uncapping in case of resting cells. We presume that the low free calcium concentration keeps on the structure of gelsolin which is able to bind actin within the cooperativity of actin bound calcium. Gelsolin can help to manage monomer pool far from the membrane and it can be linked to a basic sensory mechanism which drives the direction of filament growth in the near of the membrane.

Keywords Actin · Gelsolin · PIP2 · Isothermal kinetics

Introduction

The actin is an essential unit of the eukaryotic cytoskeleton and muscle sarcomeres with highly conservative sequences [1]. The specialized intracellular functions driven to low variety of proteins in their phylogenetic development [2–4]. Actin monomers (G-actin) and filaments (F-actin) have dynamical rearrangement thus manage cellular motility, division and transport processes [5–11]. The remodeling of actin filaments highly regulated by divalent cations (Ca^{2+} or Mg^{2+}) [12] and nucleotides (ATP, ADP) [13–20]. The stability of G-actin depends on the bound cations and nucleotides but the majority in cytoplasm is in the ATP-G-actin form [21, 22] then subsequently hydrolyses to ADP and Pi with their polymerization [13–20]. The gelsolin regulates the rearrangement of cytoskeleton [21]. After the activation of gelsolin (GSN) by calcium ions, it can sever actin filaments then capped at its barbed end. In the cytoplasm nearby of the plasma membrane, GSN manages the cellular motions and morphology by capping, severing and uncapping of F-actin [22–24]. The process of uncapping is a crucial step to help the actin polymerization with an indirect influence on the membrane remodeling. Phosphatidylinositol 4,5-bisphosphate (PIP2) is involved in signal transduction and the regulation of the actin cytoskeleton by regulation of actin-binding proteins [25–42]. GSN can bind to PIP2 [43] and thus can be localized in the near of the plasma membrane when it is released from the end of F-actin [29, 44–49]. The PIP2-binding sites on gelsolin overlaps with the ATP binding site [47, 50–52]. The structural change of gelsolin with the mechanism of uncapping is not well known but in the absence of calcium the PIP2 competes with actin for binding to GSN [46, 49, 52–54]. However, we interpreted earlier that calcium activated GSN cannot bind PIP2 [49].

✉ Dénes Lőrinczy
denes.lorinczy@aok.pte.hu

[1] Department of Biophysics, Medical School, University of Pécs, Szigeti Str. 12, Pécs 7624, Hungary

As previously shown the free calcium concentration in resting cells changing on the nanomolar level [55, 56], and in non-resting state can reach the micromolar levels [57, 58]. Cytoplasmic free magnesium levels are regulated in the nanomolar range but it does not have effect on GSN activity [49, 59, 60]. Interestingly, the reduction of calcium levels cannot cause directly the GSN release from actin, but a single calcium ion is still trapped in the complex [61]. The main concern with GSN inactivation is that it still depolymerizing actin filaments in the presence of millimolar EGTA provided nanomolar free calcium level [62, 63]. Possibly, only the PIP2 binding can fully inhibit any activity of GSN [49]. Structural rearrangement of F-actin and its binding molecules can be studied by DSC [64–66]. We probe here the isothermal enthalpy change within the interplay between GSN and F-actin under nano-, micro- and millimolar calcium concentrations and express the importance of PIP2 binding for the total inactivation of GSN. We can postulate that GSN shows remarkable thermal response to actin, addition under nanomolar calcium concentration which can be reduced by PIP2 binding.

Results

Figure 1 shows isothermal heatflow kinetics as well as the denaturation of mixing GSN with F-actin under different Ca^{2+} conditions, or in the presence of PIP2. All isotherm assays were taken 16 h but we focused on the first relevant 180 min after the relapse of the heatflow subsequently after the mixing effect, between the minimum ($\Delta Q_{initial}$) and the maximum points (ΔQ_{top}) (Fig. 1A). The heatflow was dropped down (2.4 µW) (Table 1) if 12.8 µM GSN (1 mg mL^{-1}) was added to nanomolar Ca^{2+} containing buffer then increased slowly ($1.7 \pm 0.3 \times 10^{-4}$ µW s^{-1}) in the first 3 h (Fig. 1B). In case of 46 µM F-actin (2 mg mL^{-1}) bound GSN in a ratio of 1: 3.6; under nanomolar Ca^{2+} concentration, there were two remarkable exothermic peaks. The first peak was increased quickly 9.1 ± 2.5 W in the first 15 min by the rate of $82 \pm 1.2 \times 10^{-4}$ µW s^{-1}, after a minor reduction it was followed by a second peak in 63 min. If GSN was formed complexes with 1.6 µM PIP2 [49] in the presence of nanomolar Ca^{2+} and F-actin, the heatflow was increased quickly with multiple rates (totally 4.6 ± 0.7 µW with an average rate of $17 \pm 2.5 \times 10^{-4}$ µW s^{-1}) in 65 min. Just after the isothermal processes we performed denaturation with heating rate of 0.3 K min^{-1} (Fig. 1C). GSN in the presence of nanomolar Ca^{2+} shows a main transition at 39.5 °C (Table 2). GSN and F-actin in the presence of nanomolar Ca^{2+} shows four transitions at 33, 40, 54 and 60 °C and the GSN-PIP2 complex with F-actin show three transitions at 36, 56 and 60.5 °C. PIP2 binding shifted the main peak from 33 to 36 °C, however in case of free GSN the biggest transition was observable at 39.5 °C. Figure 1D shows that the isothermal heatflow of F-actin was dropped down (endothermic 3.6 µW)(Table 1) by mixing with millimolar Ca^{2+} containing buffer then it was increased by 3.23 µW first in a quick step $100 \pm 0.8 \times 10^{-4}$ µW s^{-1} then slowly $6 \pm 1.5 \times 10^{-4}$ µWs^{-1} in the first hour. The previously described two exothermic peaks of GSN and F-actin under nanomolar Ca^{2+} were turned to be reduced in the presence of micromolar Ca^{2+}. Interestingly, we observed a minor drop (endothermic 1.36 µW) of the heatflow then it was followed by an exothermic change 3.84 ± 1.2 µW with the rate of $37 \pm 0.8 \times 10^{-4}$ µW s^{-1}. If GSN was added to F-actin in the presence of millimolar Ca^{2+}, the heatflow showed a big drop 9.7 µW at the beginning of the process then it was increased by 7.7 ± 2.8 µW with a relatively quick rate $17 \pm 1.2 \times 10^{-4}$ µW s^{-1} in the first two hours. Figure 1E shows that the shape of thermal denaturation curves in each cases from panel C seems to be Ca^{2+} dependent. F-actin in the presence of milimolar Ca^{2+} shows a main transition at 60 °C (Table 2). As we described above, the GSN and F-actin in the presence of nanomolar Ca^{2+} shows four transitions. However, in the presence of micromolar Ca^{2+}, there were multiple peaks at 45.5; 49; 53.5 and 60 °C. Under millimolar Ca^{2+}, there was only one main transition at 58 °C in case of GSN and F-actin.

Discussion and conclusions

The aim of our present work is to show thermodynamical changes due to the activation and inactivation of gelsolin. Heat flow follows the structural entropy change as increases with structural stabilization.

Under nanomolar Ca^{2+} concentration, GSN responded with a minor isothermal change to the mixing of sample. GSN addition to F-actin resulted a strong exothermic change linked to the reduction of their structural entropy. Possibly, free actin monomers were depleted by GSN binding [62, 63] which mechanism can be described as the Type I. Ca^{2+} binding sites [67] are partially saturated, and thus initialized a structural change of GSN for a cooperative binding to actin monomer. Here we found that the actin binding leads to a lower thermodynamical stability of GSN. The PIP2 binding was stabilized the structure of GSN similar to the free form with slow and weak response to the actin addition (Fig. 2). In good agreement with our previous results, since the intrinsic tryptophan of GSN responds with increased emission to PIP2 addition, the response was a less flexible structural dynamics of GSN [49]. At the end of the isotherm assays, the majority of actin was denatured around 60 °C, it can be interpreted by the hydrolyzation of ATP due to the long term processes [68].

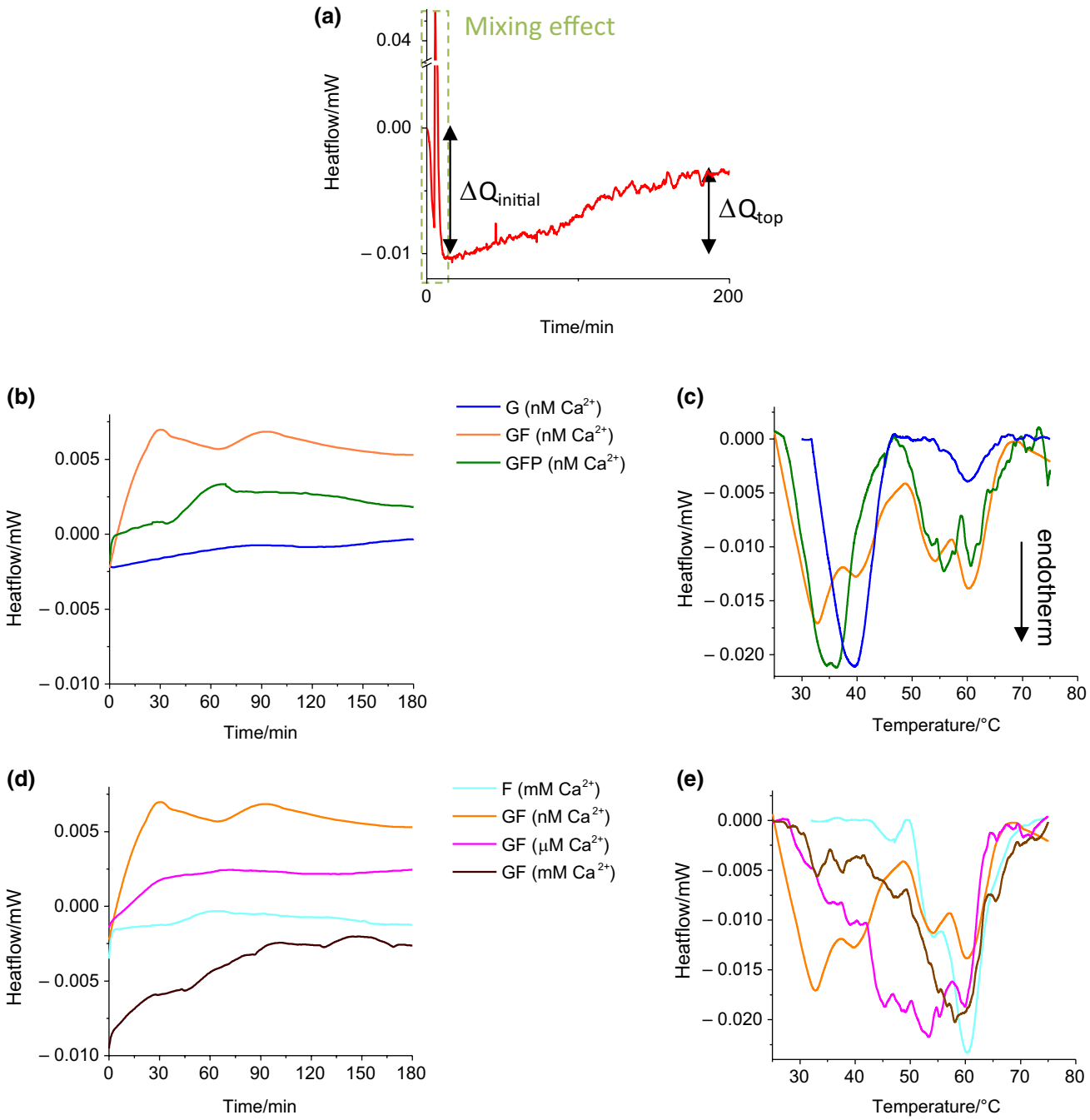

Fig. 1 Isothermal severing and capping of F-actin by GSN. **A** Schematic curve of isothermal heat flow change by the time with the mixing effect and the investigated parameters. **B** Time dependent change of isothermal heat flow in case of GSN with (light brown line /GF) or without (blue line /G) F-actin in the presence of nanomolar Ca^{2+}. The response of GSN-PIP2 complex in the presence of F-actin (green line /GFP). **C** All cases from panel B were terminated with thermal denaturation DSC scans. **D** Isothermal heat flow kinetics of F-actin in the absence (cyan line /F) or in the presence of GSN under different Ca^{2+} concentrations, nanomolar (light brown line), micromolar (magenta line) or millimolar (dark brown line). **E** Heat denaturation curves of processes from panel D. The scans are the average of three measurements, and endotherm effect is deflected downwards which is valid with all panels

Table 1 Isothermal kinetic data achieved by exponential fit to the heat flow change between the minimum and maximum value of the curves. The values are the average of three measurements

Isothermal kinetic parameters			
	k ($\times 10^{-4}$ μW s^{-1})	$\Delta Q_{initial}$ /μW	ΔQ_{top} /μW
nM			
GSN	1.7 ± 0.3	− 2.4	2.2 ± 0.5
GSN + F-actin	82 ± 1.2	− 2.2	9.1 ± 2.5
GSN + F-actin + PIP2	17 ± 2.5	− 1.2	4.6 ± 0.7
μM			
GSN + F-actin	37 ± 0.8	− 1.36	3.84 ± 1.2
mM			
GSN + F-actin	17 ± 1.2	− 9.7	7.7 ± 2.8
F-actin	100 ± 0.8; 6 ± 1.5	− 3.6	3.23 ± 0.9

Table 2 Heat denaturation parameters were collected after the end of the isothermal processes

Denaturation parameters		
	T_m/°C	ΔH_{cal}/J g^{-1}
nM		
GSN	39.5	0.058 ± 0.0006
GSN + F-actin	33; 40; 54; 60	0.045 ± 0.003
GSN + F-actin + PIP2	36; 56; 60.5	0.04 ± 0.0032
μM		
GSN + F-actin	45.5; 49; 53.5; 60	0.054 ± 0.0065
mM		
GSN + F-actin	58	0.04 ± 0.0036
F-actin	60	0.038 ± 0.0019

Under micromolar Ca^{2+} concentration, the Ca^{2+} binding to Type II. binding sites [67] were initialized structural change of GSN and the mixing of sample can make fragments of long actin filaments and all newly exposed barbed end can be quickly capped by the partially active GSN. However, a slow structural transition in all capped actin filaments was observable.

Under millimolar Ca^{2+} concentration, the fully active GSN can do very fast severing within the mixing of the sample and induced a relatively big endotherm drop of the heat flow at the beginning of the process. Then subsequently, there was a relatively slow exotherm change which can be explained by the capping and within caused slow structural rearrangement of short filaments. However, if we mixed F-actin with buffer only it shows a very fast then a very slow isothermal process, possibly it was a recovery after certain fragmentations. As Nag et al.

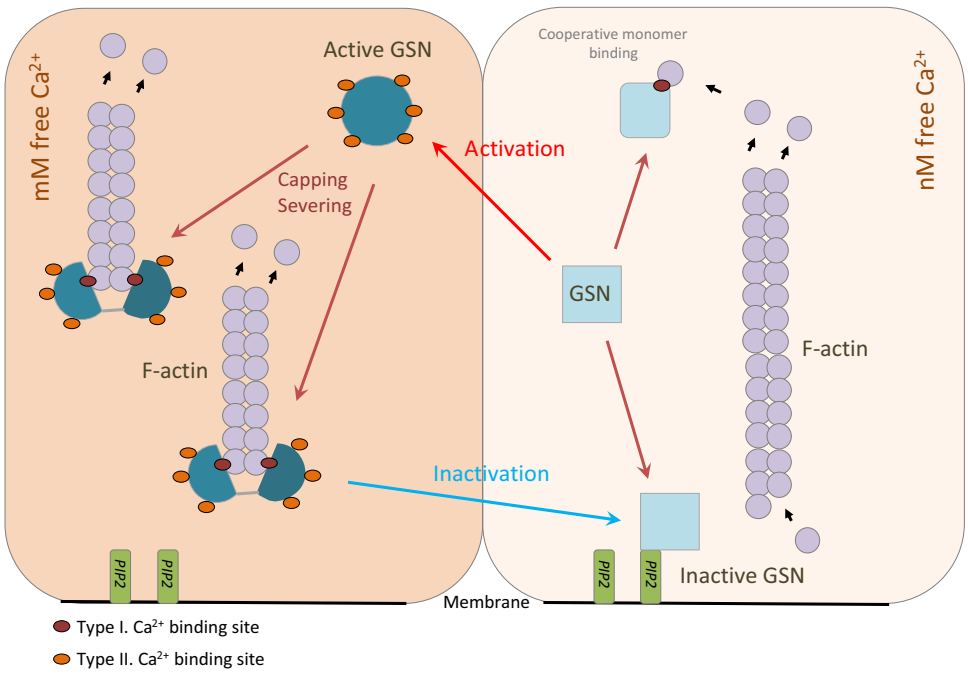

Fig. 2 Schematic model of calcium induced GSN activation in the near of the plasma membrane

published in 2009 [69] the transition temperature of GSN domains was increased from 35 to 60 °C with the change of nanomolar to millimolar Ca^{2+} concentration. Here we found that the heat denaturation of actin-GSN shows two main components nearby 30 °C and 60 °C in the presence of nanomolar, multiple peaks between 30 and 60 °C in the presence of micromolar and one main component nearby 60 °C in the presence of millimolar Ca^{2+}. What we can interpret as the GSN domains were turned to be more compact by the calcium binding which were connected together by flexible linkers seems like beads on string.

Here we have demonstrated that PIP2 binding stabilized the whole structure of gelsolin and possibly reduced its actin monomer binding activity under nanomolar calcium as the typical cytoplasmic calcium concentration of resting cells. If gelsolin-capped filaments point at the plasma membrane, the local concentration of gelsolin increases by forming PIP2 clusters [70]. All the conditions which help the binding between gelsolin and PIP2, and hence, filament uncapping in case of resting cells. The total inactivation of gelsolin is required PIP2.

We can presume that the low free calcium concentration keeps on the structure of gelsolin which is able to bind actin within the cooperativity of actin bound calcium (Fig. 2). Gelsolin can help to manage monomer pool far from the membrane and it can be linked to a basic sensory mechanism which influences the direction of filament growth in the near of the membrane.

Materials and methods

Proteins

His-tagged human wild-type gelsolin was expressed in *E*. coli strain Rosetta2 (DE3) pLysS cells from a pSY5 plasmid [71]. The protein was subjected to Ni-NTA affinity chromatography, HRV 3C protease cleavage, followed by gel filtration (Superdex 200, GE Healthcare) in 10 mM MOPS, 150 mM NaCl, pH 8. Traces of calcium were removed by dialysis (4 mM MOPS, 1 mM EGTA, pH 7.4, overnight). Rabbit skeletal muscle actin was prepared from acetone powder by a modified protocol from Spudich and Watt [72]. Actin was stored in buffer A (4 mM MOPS, 0.2 mM ATP (ATP disodium trihydrate, Sigma-Aldrich), 0.1 mM $CaCl_2$, pH 7.4). We applied 2 mM EGTA then 2 mM $MgCl_2$. Actin polymerization process was initialized by addition of 100 mM KCl following the same protocol as in our previous study [64]. 12.8 µM gelsolin was incubated under physiological salt conditions (100 µM $CaCl_2$, 100 mM KCl, 1 mM $MgCl_2$, 0.2 mM ATP, 4 mM MOPS, pH 7.4) supplemented with EGTA or $CaCl_2$ to vary the free calcium levels (calculated with Maxchelator Stanford); for nM: 2 mM EGTA; for µM: 100 µM EGTA; for mM: 1 mM $CaCl_2$. We used 1.6 µM PIP2 (PtdIns-(3,5)-P2(1,2-Dihexanoyl), Cayman Chemicals) which is below the CMC of PIP2 [73–75], incubated with F-actin in the presence of 2 mM EGTA.

DSC measurements

The actin samples were freshly prepared before all measurements. The isotherm kinetics analysis was made by a SETARAM Micro-DSCII calorimeter on room temperature, 22 °C for 16 h. After the third hour of measurements, we observed the continuous dropping of heat flow which can be described by the decay of ATP and actin filaments. We used Hastelloy designed pair of "mixing batch" vessels for isotherm measurements ($V_{lower} = 500$ µL, $V_{upper} = 200$ µL) in the reference vessel the GSN was mixed with buffer only and in the sample one with F-actin in the presence of nanomolar, micromolar or millimolar free Ca^{2+} (calculated by MaxChelator, https://somapp.ucdmc.ucdavis.edu) and after it subsequently undergone for denaturation measurements. Kinetics measurements were carried out with an isotherm program then finally denatured by heating up them with 0.3 K/min up to 80 °C. MOPS buffer was used as a reference. The reference and sample vessels were equilibrated with a precision of ± 0.1 mg; this way we did not need to do any correction between vessels' heat capacity. The first point of our analysis was the minimum of the heat flow change ($\Delta Q_{initial}$) after a single sharp peak which shows the mixing effect, and thus the curve was increased slowly to the maximum point (ΔQ_{top}) (Fig. 1A). The exponential fitting resulted the time rate (k) of the peaks, the measurements were started in 5 min after reaching the thermal equilibrium between the vessels, but we used for the analysis the part of the curve after the mixing effect. Actin and gelsolin based molecular events were happened only in the first three hours then all curves decreased slowly possibly by the decay of ATP thus the most reasonable time duration of kinetics was analyzed in the first 10,800 s. All kinetic processes were terminated with heat denaturation assays. With the help of a two-point SETARAM peak integration setting, the denaturation calorimetric enthalpy was calculated from the area under the heat absorption curve, and then, the results [denaturation or melting temperature (T_m) and calorimetric enthalpy (ΔH_{cal}) data of samples] were compared. This method is identical with the protocol as we applied in our previous study [64].

Acknowledgements This work was supported by CO-272 (OTKA) grant (DL) and supported by University of Pécs, Medical School, grant of Dr. Szolcsányi János Research Fund (ÁOK-KA) (DS).

Author's contribution DS: rising the problem, sample preparation and handling, data analysis, manuscript writing. DL: corresponding author, principal investigator, DSC experiments, data analysis, manuscript writing.

Funding Open access funding provided by University of Pécs.

Data availability There are no additional available data to upload.

Declarations

Conflict of interest The authors declare that they have no known competing financial interests or personal relationships that could have appeared to influence the work reported in this paper.

Consent for publication Copyright form has been uploaded with the manuscript.

References

1. Hardin J, Bertoni G, Kleinsmith LJ. Becker's World of the Cell. New York: Pearson 8th ed. 2015. pp. 422–446.
2. Ono S. Dynamic regulation of sarcomeric actin filaments in striated muscle. Cytoskel. 2010;67:677–92.
3. Sanger JW, Wang J, Fan Y, White J, Mi-Mi L, Dube DK, Sanger JM, Pruyne D. Assembly and Maintenance of Myofibrils in Striated Muscle. Handb. Exp. Pharmacol. 2017; 39–75.
4. Gunning PW, Ghoshdastider U, Whitaker S, Popp D, Robinson RC. The evolution of compositionally and functionally distinct actin filaments. J Cell Sci. 2015;128:2009–19.
5. Cossart P. Actin-based bacterial motility. Curr Opin Cell Biol. 1996;7:94–101.
6. Steinmetz MO, Stoffler D, Hoenger A, Bremer A, Aebi U. Actin: from cell biology to atomic detail. J Struct Biol. 1997;119:295–320.
7. Pollard TD, Blanchoin L, Mullins RD. Molecular mechanisms controlling actin filament dynamics in nonmuscle cells. Ann Rev Biophys Biomol Struc. 2000;29:545–76.
8. Pollard TD, Borisy GG. Cellular motility driven assembly and dissembly of actin filaments. Cell. 2003;112:453–65.
9. Carlier M-F, Le Clainche C, Wiesner S, Pantolini D. Actin-based motility: from molecules to movement. BioEss. 2003;25:336–45.
10. Pantolini D, Le Clainche C, Carlier M-F. Mechanism of actin-based motility. Science. 2001;292:1502–6.
11. Hehnly H, Stamnes M. Regulating cytoskeleton-based vesicle motility. FEBS L. 2007;581:2112–8.
12. Sheterline P, Clayton J, Sparrow J. Actin. Protein Profile. 1995;2:1–103.
13. Feuer G, Molnár F, Pettko E, Straub FB. Studies on the composition and polymerization of actin. Hung Acta Physiol. 1948;1(4–5):150–63.
14. Pollard TD. Rate constants for the reactions of ATP- and ADP-actin with the ends of actin filaments. J Cell Biol. 1986;103:2747–54.
15. Carlier M-F, Pantolini D. Direct evidence for ADP-Pi-F-actin as the major intermediate in ATP-actin polymerization. rate of dissociation of Pi from actin filaments. Biochem. 1986;25:7789–92.
16. Korn ED, Carlier M-F, Pantaloni D. Actin polymerization and ATP hydrolysis. Science. 1987;238:638–44.
17. Carlier M-F. Role of nucleotide hydrolysis in the polymerization of actin and tubulin. Cell Biophys. 1988;12:105–17.
18. Carlier M-F, Pantolini D. Binding of phosphate to F-ADP-actin and role of F-ADP-P(i)-actin in ATP-actin polymerization. J Biol Chem. 1988;263:817–25.
19. Janmey PA, Hvidt S, Oster GF, Lamb J, Stossel TP, Hartwig JH. Effect of ATP on actin filament stiffness. Nature. 1990;347:95–9.
20. Pollard TD, Goldberg I, Schwarz WH. Nucleotide exchange, structure, and mechanical properties of filaments assembled from ATP-actin and ADP-actin. J Biol Chem. 1992;267:20339–45.
21. Nag S, Larsson M, Robinson RC, Burtnick LD. Gelsolin: the tail of a molecular gymnast. Cytoskel. 2013;70(7):360–84.
22. Hartwig JH, Chambers KA, Stossel TP. Association of gelsolin with actin filaments and cell membranes of macrophages and platelets. J Cell Biol. 1989;108(2):467–79.
23. Allen PG. Actin filament uncapping localizes to ruffling lamellae and rocketing vesicles. Nat Cell Biol. 2003;5(11):972–9.
24. Cooper JA, Loftus DJ, Frieden C, Bryan J, Elson EL. Localization and mobility of gelsolin in cells. J Cell Bio. 1988;106(4):1229–40.
25. Yin HL, Janmey PA. Phosphoinositide regulation of the actin cytoskeleton. Annu Rev Physiol. 2003;65:761–89.
26. Janmey PA. Phosphoinositides and calcium as regulators of cellular actin assembly and disassembly. Annu Rev Physiol. 1994;56:169–91.
27. Schafer DA, Cooper JA. Control of actin assembly at filament ends. Annu Rev Cell Dev Biol. 1995;11:497–518.
28. Hilpela P, Vartiainen MK, Lappalainen P. Regulation of the actin cytoskeleton by PI(4,5)P2 and PI(3,4,5)P3. Curr Top Microbiol Immunol. 2004;282:117–63.
29. Janmey PA, Stossel TP. Modulation of gelsolin function by phosphatidylinositol 4,5-bisphosphate. Nature. 1987;325(6102):362–4.
30. Yu FX, Johnston PA, Sudhof TC, Yin HL. gCap39, a calcium ion- and polyphosphoinositide-regulated actin capping protein. Science. 1990;250(4986):1413–5.
31. Schafer DA, Jennings PB, Cooper JA. Dynamics of capping protein and actin assembly in vitro: uncapping barbed ends by polyphosphoinositides. J Cell Biol. 1996;135(1):169–79.
32. Lassing I, Lindberg U. Specific interaction between phosphatidylinositol 4,5-bisphosphate and profilactin. Nature. 1985;314(6010):472–4.
33. Yonezawa N, Nishida E, Iida K, Yahara I, Sakai H. Inhibition of the interactions of cofilin, destrin, and deoxyribonuclease I with actin by phosphoinositides. J Biol Chem. 1990;265(15):8382–6.
34. Palmgren S, Ojala PJ, Wear MA, Cooper JA, Lappalainen P. Interactions with PIP2, ADP-actin monomers, and capping protein regulate the activity and localization of yeast twinfilin. J Cell Biol. 2001;155(2):251–60.

35. Higgs HN, Pollard TD. Activation by Cdc42 and PIP(2) of Wiskott-Aldrich syndrome protein (WASp) stimulates actin nucleation by Arp2/3 complex. J Cell Biol. 2000;150(6):1311–20.
36. Miki H, Miura K, Takenawa T. N-WASP, a novel actin-depolymerizing protein, regulates the cortical cytoskeletal rearrangement in a PIP2-dependent manner downstream of tyrosine kinases. EMBO J. 1996;15(19):5326–35.
37. Schafer DA, Weed SA, Binns D, Karginov AV, Parsons JT, Cooper JA. Dynamin2 and cortactin regulate actin assembly and filament organization. Curr Biol CB. 2002;12(21):1852–7.
38. Fukami K, Furuhashi K, Inagaki M, Endo T, Hatano S, Takenawa T. Requirement of phosphatidylinositol 4,5-bisphosphate for alpha-actinin function. Nature. 1992;359(6391):150–2.
39. Furuhashi K, Inagaki M, Hatano S, Fukami K, Takenawa T. Inositol phospholipid-induced suppression of F-actin-gelating activity of smooth muscle filamin. Biochem Biophys Res Com. 1992;184(3):1261–5.
40. Stock A, Steinmetz MO, Janmey PA, Aebi U, Gerisch G, Kammerer RA, Weber I, Faix J. Domain analysis of cortexillin I: actin-bundling, PIP(2)-binding and the rescue of cytokinesis. EMBO J. 1999;18(19):5274–84.
41. Gilmore AP, Burridge K. Regulation of vinculin binding to talin and actin by phosphatidyl-inositol-4-5-bisphosphate. Nature. 1996;381(6582):531–5.
42. Hirao M, Sato N, Kondo T, Yonemura S, Monden M, Sasaki T, et al. Regulation mechanism of ERM (ezrin/radixin/moesin) protein/plasma membrane association: possible involvement of phosphatidylinositol turnover and Rho-dependent signaling pathway. J Cell Biol. 1996;135(1):37–51.
43. Chou J, Stolz DB, Burke NA, Watkins SC, Wells A. Distribution of gelsolin and phosphoinositol 4,5-bisphosphate in lamellipodia during EGF-induced motility. Int J Biochem Cell Bio. 2002;34(7):776–90.
44. Janmey PA, Matsudaira PT. Functional comparison of villin and gelsolin. Effects of Ca^{2+}, KCl, and polyphosphoinositides. J Biol Chem. 1988;263(32):16738–43.
45. Maekawa S, Sakai H. Inhibition of actin regulatory activity of the 74-kDa protein from bovine adrenal medulla (adseverin) by some phospholipids. J Biol Chem. 1990;265(19):10940–2.
46. Janmey PA, Lamb J, Allen PG, Matsudaira PT. Phosphoinositide-binding peptides derived from the sequences of gelsolin and villin. J Biol Chem. 1992;267(17):11818–23.
47. Feng L, Mejillano M, Yin HL, Chen J, Prestwich GD. Full-contact domain labeling: identification of a novel phosphoinositide binding site on gelsolin that requires the complete protein. Biochem. 2001;40(4):904–13.
48. Hartwig JH, Bokoch GM, Carpenter CL, Janmey PA, Taylor LA, Toker A, Stossel TP. Thrombin receptor ligation and activated Rac uncap actin filament barbed ends through phosphoinositide synthesis in permeabilized human platelets. Cell. 1995;82(4):643–53.
49. Szatmári D, Xue B, Kannan B, Burtnick LD, Bugyi B, Nyitrai M, Robinson RC. ATP competes with PIP2 for binding to gelsolin. PLoS ONE. 2018;13(8):e0201826.
50. Tuominen EK, Holopainen JM, Chen J, Prestwich GD, Bachiller PR, Kinnunen PK, Jamney PA. Fluorescent phosphoinositide derivatives reveal specific binding of gelsolin and other actin regulatory proteins to mixed lipid bilayers. Euro J Biochem. 1999;263(1):85–92.
51. Banno Y, Nakashima T, Kumada T, Ebisawa K, Nonomura Y, Nozawa Y. Effects of gelsolin on human platelet cytosolic phosphoinositide-phospholipase C isozymes. J Biol Chem. 1992;267(10):6488–94.
52. Liepina I, Czaplewski C, Janmey P, Liwo A. Molecular dynamics study of a gelsolin-derived peptide binding to a lipid bilayer containing phosphatidylinositol 4,5-bisphosphate. Biopol. 2003;71(1):49–70.
53. Urosev D, Ma Q, Tan AL, Robinson RC, Burtnick LD. The structure of gelsolin bound to ATP. J Mol Biol. 2006;357(3):765–72.
54. Burtnick LD, Koepf EK, Grimes J, Jones EY, Stuart DI, McLaughlin PJ, Robinson RC. The crystal structure of plasma gelsolin: implications for actin severing, capping, and nucleation. Cell. 1997;90(4):661–70.
55. Maravall M, Mainen ZF, Sabatini BL, Svoboda K. Estimating intracellular calcium concentrations and buffering without wavelength ratioing. Biophys J. 2000;78(5):2655–67.
56. Baffy G, Varga Z, Foris G, Leovey A. Disturbed intracellular calcium-related processes of hepatocytes and neutrophils in human alcoholic liver disease. Clin Biochem. 1990;23(3):241–5.
57. Saqr HE, Guan Z, Yates AJ, Stokes BT. Mechanisms through which PDGF alters intracellular calcium levels in U-1242 MG human glioma cells. Neurochem Int. 1999;35(6):411–22.
58. Nohutcu RM, McCauley LK, Horton JE, Capen CC, Rosol TJ. Effects of hormones and cytokines on stimulation of adenylate cyclase and intracellular calcium concentration in human and canine periodontal-ligament fibroblasts. Arch Oral Biol. 1993;38(10):871–9.
59. McCarthy J, Kumar R. Divalent cation metabolism: calcium. In: Schrier R, Berl T, editors. Atlas of Diseases of the Kidney 1. Curr Med. 1999;4.1–4.8
60. Murphy E. Mysteries of magnesium homeostasis. Circ Res. 2000;86(3):245–8.
61. Bryan J, Kurth MC. Actin-gelsolin interactions. Evidence for two actin-binding sites. J Biol Chem. 1984;259(12):7480–7.
62. Vemula V, Huber T, Ušaj M, Bugyi B, Månsson A. Myosin and gelsolin cooperate in actin filament severing and actomyosin motor activity. J Biol Chem. 2021;296:100181.
63. Singaravelu P, Lee WL, Wee S, Ghoshdastider U, Ding K, Gunaratne J, Grimes JM, Swaminathan K, Robinson RC. Yersinia effector protein (YopO)-mediated phosphorylation of host gelsolin causes calcium-independent activation leading to disruption of actin dynamics. J Biol Chem. 2017;292(19):8092–100.
64. Farkas P, Szatmári D, Könczöl F, Lőrinczy D. Cyclophosphamide treatment evoked side effect on skeletal muscle actin, monitored by DSC. J Therm Anal Calorim. 2022;147:3609–14.
65. Lőrinczy D, Könczöl F, Gaszner B, Belágyi J. Structural stability of actin as studied by DSC and EPR. Thermochim Acta. 1998;322:95–100.
66. Lőrinczy D. Thermal analysis in biological and medical applications. J Therm Anal Calorim. 2017;130:1263–80.
67. Choe H, Burtnick LD, Mejillano M, Yin HL, Robinson RC, Choe S. The calcium activation of gelsolin: insights from the 3Å structure of the G4–G6/actin complex. J Mol Bio. 2002;324(4):691–702.
68. Dudás R, Kupi T, Vig A, Orbán J, Lőrinczy D. Effect of phalloidin on the skeletal muscle ADP-actin filaments. J Therm Anal Calorim. 2009;95:709–12.
69. Nag S, Ma Q, Wang H, Chumnarnsilpa S, Lee WL, Larsson M, Kannan B, Hernandez-Valladares M, Burtnick LD, Robinson RC. Ca2+ binding by domain 2 plays a critical role in the activation and stabilization of gelsolin. Proc Natl Acad Sci USA. 2009;106(33):13713–8.
70. Wang J, Richards DA. Segregation of PIP2 and PIP3 into distinct nanoscale regions within the plasma membrane. Biol Open. 2012;1(9):857–62.
71. Wang H, Chumnarnsilpa S, Loonchanta A, Li Q, Kuan YM, Robine S, Larsson M, Mihalek I, Burtnick LD, Robinson RC. Helix straightening as an activation mechanism in the

gelsolin superfamily of actin regulatory proteins. J Biol Chem. 2009;284(32):21265–9.
72. Spudich JA, Watt S. The regulation of rabbit skeletal muscle contraction I Biochemical studies of the interaction of the tropomyosin-troponin complex with actin and the proteolytic fragments of myosin. J Biol Chem. 1971;246(15):4866–71.
73. Moens PDJ, Bagatolli LA. Profilin binding to sub-micellar concentrations of phosphatidylinositol (4,5) bisphosphate and phosphatidylinositol (3,4,5) trisphosphate. BBA-Biom. 2007;1768(3):439–49.
74. Salanci E, Malík I, Šandrik R, Pecher D, Andriamainty F. Determination of the critical micelle concentration and thermodynamic parameters of phenylcarbamic acid derivatives using a fluorescence method. Chem Pap. 2021;75:3081–90.
75. Janmey PA, Iida K, Yin HL, Stossel TP. Polyphosphoinositide micelles and polyphosphoinositide-containing vesicles dissociate endogenous gelsolin-actin complexes and promote actin assembly from the fast-growing end of actin filaments blocked by gelsolin. J Biol Chem. 1987;262(25):12228–36.